Macromolecules

Volume 26, Number 12 June 7, 1993

Novel Photo-Cross-Linkable Liquid Crystalline Polymers: Poly[bis(benzylidene)] Esters

Gangadhara and Kaushal Kishore*

Department of Inorganic and Physical Chemistry, Indian Institute of Science, Bangalore 560 012, India

Received May 4, 1992; Revised Manuscript Received February 8, 1993

ABSTRACT: A new class of photo-cross-linkable main-chain liquid crystalline polymers (PMCLCPs) containing bis(benzylidene)cycloalkanone groups have been synthesized and studied for their liquid crystalline and photochemical properties. The bis(benzylidene)cycloalkanone group in the chain functions both as a mesogen and as a photoreactive center. All of the polymers exhibit a nematic mesophase. Two kinds of photoreactions, namely, photoisomerization and photo-cross-linking, operate in these polymers. Above T_g, at the initial stages of irradiation, photoisomerization predominates the cross-linking, which results in the disruption of the chromophore aggregates. Below T_g, because of the restricted mobility of the chains, only cross-linking takes place. Studies on the model compound, bis(benzylidene)cyclopentanone, confirm the above observations and demonstrate further that the cross-linking proceeds by the $2\pi + 2\pi$ cycloaddition reaction of the bis(benzylidene)cycloalkanone moieties. The cross-linking rate decreases with increase in the size of the cycloalkanone ring. Heating the solution cast polymer film results in the ordered aggregation of the chromophores just above T_g and also at the crystal to crystal transition temperature, which facilitates the photo-cross-linking reactions. In the isotropic phase, the random orientation of the chromophores drastically curtails the cross-linking rate.

Introduction

Since their discovery[1] in 1975, liquid crystalline polymers (LCPs) have gained considerable interest for their integrated properties of polymers and low molar mass liquid crystals.[2-4] The chemically cross-linked network of such polymers possesses fascinating anisotropic mechanical, electrical, and optical properties suitable for technological applications.[5-15] There are two kinds of liquid crystalline (LC) networks, namely the LC elastomers and LC thermosets. LC elastomers combine the properties of mesogens and conventional elastomers. They are lightly cross-linked materials with cross-linking density of less than 10%. The end product is usually a multidomain LCP, which can subsequently be aligned under tension to produce anisotropic network structure. The LC thermosets, on the other hand, are densely cross-linked materials like the normal thermosets imbibing the anisotropic properties of liquid crystals. They usually have a cross-linking density of more than 90%, and the chains are uniformly oriented in the network.

These network systems are made by two main procedures. The one-step procedure involves the simultaneous formation of the linear polymer chains and the cross-links. For making LC elastomers, this method consists of the polymerization of a mixture of mesogenic monomer and bifunctional cross-linking agent in a solvent.[15] For preparing LC thermosets by this method, a mesogenic bifunctional monomer, homogeneously aligned by external field or by special surface treatment, is subjected to polymerization.[16-18] In the two-step procedure, commonly used for LC elastomers, a linear mesogenic or nonmesogenic polymer containing reactive centers is first synthesized. The subsequent step involves the cross-linking of the chains merely by connecting these reactive centers when the linear polymer is mesogenic.[19-23] For nonmesogenic linear polymers, cross-linking and introduction of mesogenic units are done simultaneously in the second step.[24,25] The cross-linking reactions in these two procedures can be induced by thermal or photochemical methods. The photochemical methods are preferred, particularly for films and coatings, because the reaction rates can be easily controlled just by changing the intensity of the radiation. Moreover, the cross-linking reaction can be effected almost at any desired temperature, orientation, and configuration.[5,18,26] Further, the selection of reaction temperature allows the order parameter and the refractive indices of the resulting network to be adjusted.[27]

Linear LCPs, containing photo-cross-linkable groups, besides their common use in making anisotropic networks, as discussed above, have attracted considerable attention

0024-9297/93/2226-2995$04.00/0

Scheme I. Preparation of Poly[bis(benzylidene)] Esters

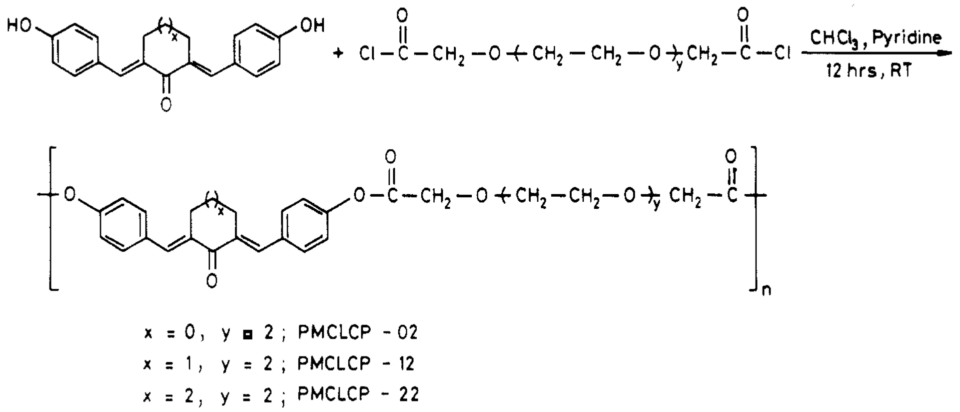

in other areas, like information storage,[28,29] nonlinear optics,[30] photochemical reactions in organized environment,[31,32] and permeation of gases and drugs through the aligned membranes.[33,34] All of these liquid crystalline polymers contain cinnamate ester groups, which undergo photodimerization leading to the cross-linking of the polymer chains.[35-38] In this paper, we present a new class of photo-cross-linkable main-chain liquid crystalline polymers (PMCLCPs), which contain photoactive bis(benzylidene)cycloalkanone groups. Studies on their synthesis, structural characterization, mesomorphic behavior, and photochemical properties are the main focus of this paper.

Experimental Section

Materials. *p*-Hydroxybenzaldehyde, cycloheptanone, tetraethylene glycol, and $BF_3(Et_2O)$ were obtained from Merck-Schuchart and used without further purification. Cyclohexanone, benzaldehyde, and the solvents were purified by distillation.

Synthesis. Cyclopentanone was prepared from adipic acid using barium hydroxide as a catalyst.[39] **Bis(benzylidene)cyclopentanone** was synthesized by refluxing a mixture of 1:2 molar ratio of cyclopentanone and benzaldehyde in 1% NaOH solution. To prepare the **photodimer of bis(benzylidene)cyclopentanone,** 1.0 g of finely powdered compound was smeared uniformly over a 15 × 15 cm glass plate and irradiated with a 125-W medium-pressure mercury lamp for 24 h. The dimer was separated by silica gel column using 1:2 ethyl acetate and hexane as eluent. Yield 0.53 g (53%); mp 226 °C; IR (KBr) 1703 ($\nu_{C=O}$), 1607 ($\nu_{C=C}$) cm^{-1}; ^{1}H NMR ($CDCl_3$, TMS) δ 7.59–7.04 (m, 22 H, aromatic and –CH=), 4.43 (s, 2 H, protons on the cyclobutane ring), 2.72–2.36 (m, 4 H, –CH$_2$–, β to the keto group on the cyclopentanone ring), 2.41–2.36 (m, 4 H, –CH$_2$–, γ to the keto group of the cyclopentanone ring).

Bis(4-hydroxybenzylidene)cyclopentanone. A mixture of 4.21 g (0.05 mol) of cyclopentanone and 12.21 g (0.1 mol) of *p*-hydroxybenzaldehyde was dissolved in 25 mL of absolute ethanol. This solution was refluxed for 4 h after 3 drops of $BF_3(Et_2O)$ was added. The reaction mixture was then cooled to 0 °C, and the crystallized product was filtered and washed with cold ethanol. Recrystallization from methanol yielded fine yellow crystals. Yield 12.7 g (87%); mp 391.6 °C; IR (KBr) 3400 (ν_{O-H}), 1666 ($\nu_{C=O}$), 1599 ($\nu_{C=C}$) cm^{-1}; ^{1}H NMR (DMSO-d_6, TMS) δ 3.02 (s, 4 H, –CH$_2$–, β to the keto group of cyclopentanone), 6.87 (d, 4 H, aromatic), 7.33 (s, 2 H, –CH=), 7.54 (d, 4 H, aromatic), 10.06 (s, 2 H, –OH).

Bis(4-hydroxybenzylidene)cyclohexanone. This monomer was also prepared according to the same procedure used for bis(4-hydroxybenzylidene)cyclopentanone. Recrystallization from a 3:1 mixture of methanol and water yielded fine yellowish green crystals. Yield 12.8 g (84%); mp 282 °C; IR (KBr) 3380 (ν_{O-H}), 1669 ($\nu_{C=O}$), 1595 ($\nu_{C=C}$) cm^{-1}; ^{1}H NMR (DMSO-d_6, TMS) δ 1.68 (s, 4 H, γ to the keto group of the cyclohexanone), 2.83 (s, 4 H, β to keto group of the cyclohexanone), 6.84 (d, 4 H, aromatic), 7.55 (s, 2 H, –CH=), 7.45 (d, 4 H, aromatic), 9.95 (s, 2 H, –OH).

Bis(4-hydroxybenzylidene)cycloheptanone. To a mixture of 1.21 g (0.01 mol) of cycloheptanone and 2.44 g (0.02 mol) of *p*-hydroxybenzaldehyde was added dropwise 3 mL of dry piperidine so that the temperature did not rise above 40 °C. After the addition was complete, the mixture was stirred at 80 °C for 6 h. Subsequently, it was diluted with 15 mL of pyridine and poured into 250 mL of cold water. The solution was then acidified with HCl, and the separated yellow solid was filtered. Recrystallization from a 3:1 mixture of methanol and water yielded fine light green crystals. Yield 2.5 g (78%); mp 252 °C; IR (KBr) 3360 (ν_{O-H}, phenolic), 1654 ($\nu_{C=O}$, keto), 1604 ($\nu_{C=C}$, olefinic) cm^{-1}; ^{1}H NMR (DMSO-d_6, TMS) δ 1.83 (s, 4 H, –CH$_2$–, γ to the keto group of cycloheptanone ring), 2.6 (s, 4 H, –CH$_2$–, β to the keto group of the cycloheptanone), 6.83 (d, 4 H, aromatic), 7.14 (s, 2 H, –CH=), 7.36 (d, 4 H, aromatic), 9.84 (s, 2 H, –OH).

Tetragolic Acid. This dicarboxylic acid was derived from tetraethylene glycol by oxidizing with concentrated HNO_3. To 100 g of HNO_3 (d = 1.4) was added, 5.0 g of tetraethylene glycol and the mixture was heated slowly until it began to evolve nitrous oxide vapors at about 80 °C. The mixture was then cooled to 45 °C, and an additional 15 g of tetraethylene glycol was added in a dropwise manner such that the reaction proceeds with the evolution of nitrous oxide vapors while the temperature is maintained between 45 and 50 °C. After the addition was complete, the mixture was stirred at 45 °C for 3 h and at 80 °C for 30 min. It was then dried under vacuum at 70 °C for 3 h. The viscous mass thus obtained was dissolved in 25 mL of acetone and poured into 150 mL of benzene. The tetragolic acid, separated as a brown viscous liquid, was further dried by azeotropic distillation with benzene using a Dean–Stark apparatus for 12 h. Yield 21 g (92%); IR (KBr) 4374 (ν_{O-H}), 1736 ($\nu_{C=O}$), 1139 (ν_{CH_2O}) cm^{-1}; ^{1}H NMR (DMSO-d_6, TMS) δ 3.95 (4 H, s, –O–CH$_2$–COO–), 3.48–3.5 (8 H, M, –O–CH$_2$–CH$_2$–O–).

Tetragolic Acid Dichloride. Tetragolic acid (15 g, 0.07 mol) and 30 g (0.23 mol) of oxalyl chloride were stirred in 100 mL of benzene containing 3 drops of pyridine for 24 h at room temperature. After the completion of the reaction, benzene was removed under vacuum at 50 °C. Tetragolic acid dichloride thus obtained was distilled at reduced pressure to give a colorless liquid, bp 140 °C/1mmHg, yield 97%. IR (KBr) 1803 ($\nu_{C=O}$), 1145 (ν_{CH_2O}) cm^{-1}; ^{1}H NMR ($CDCl_3$, TMS) δ 3.69–3.9 (M, 8 H, –O–CH$_2$–CH$_2$–O–), 4.52 (s, 4 H, –O–CH$_2$–COO–).

Polymerization. All of the polymers were prepared according to the same general procedure (Scheme I); a typical synthesis of PMCLCP-12 is described below.

Bis(4-hydroxybenzylidene)cyclohexanone (3.72 g, 12.2×10^{-3} mol) was dissolved in 10 mL of dry pyridine, and the solution was cooled to 0 °C. To this solution was added dropwise 3.41 g (12.2×10^{-3} mol) of tetragolic acid dichloride in chloroform. After the completion of the addition, the solution was stirred at room temperature for 24 h and the mixture was poured into 150 mL of methanol. The precipitated polymer was filtered off, purified by reprecipitation, and dried under vacuum, yield 5.4 g (84%).

Measurements. The intrinsic viscosity ([η]) of the polymers was measured in pyridine using a Schott–Geratte Ubbelohde viscometer at 30 °C. ^{1}H NMR spectra were recorded on a 400-MHz Bruker AMX-400 FTNMR spectrometer using chloroform-d and dimethyl-d_6 sulfoxide as solvents. The chemical shifts were calibrated using tetramethylsilane (TMS). Infrared spectra were recorded on a Bio-Rad FTS 7 FTIR spectrophotometer

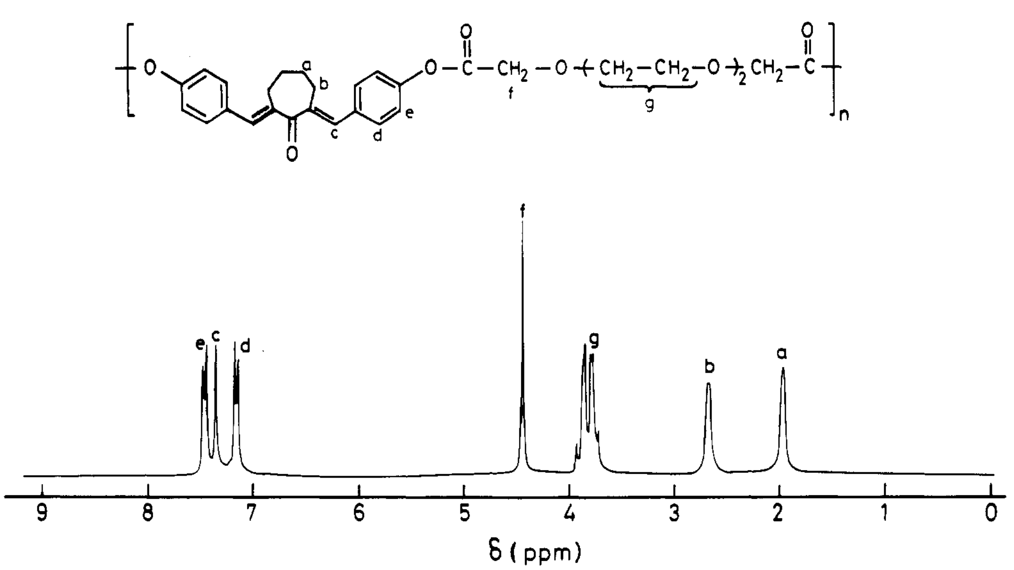

Figure 1. Representative 400-MHz ^1H NMR spectrum of PMCLCP-22 in $CDCl_3$.

Table I. Yield, Viscosity, and IR Data for the Polymers

			IR absorption band, cm^{-1}		
polymer	yield	[η]	$\nu_{C=O}$, ester	$\nu_{C=O}$, keto	$\nu_{C=C}$, olefinic
PMCLCP-02	76	0.08[a]	1740	1660	1570
PMCLCP-12	85	0.15[b]	1750	1645	1583
PMCLCP-22	81	0.11[b]	1745	1645	1585

[a] c = 0.5 g/dL in pyridine at 25 °C. [b] c = 1.0 g/dL in pyridine at 25 °C.

Table II. ^1H NMR Chemical Shift Values and Assignments for the Polymers

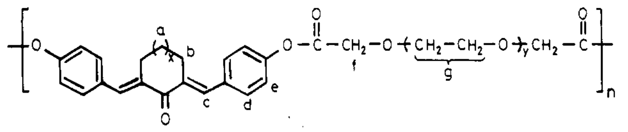

	^1H NMR chemical shift, ppm						
polymer	a	b	c	d	e	f	g
PMCLCP-02		3.08	3.82	4.77	7.18	7.55	7.45
PMCLCP-12	1.88	2.93	3.85	4.49	7.17	7.49	7.76
PMCLCP-22	1.97	2.68	3.82	4.44	7.15	7.45	7.36

using KBr pellets. UV absorption spectra were recorded on a Hitachi U-3400 spectrophotometer. A Du Pont TA9900 differential scanning calorimeter (DSC) was used to determine the thermal transitions, which were read maxima and minima of the endothermic and exothermic peaks, respectively. The glass transition temperature (T_g) is taken as the middle point of the heat capacity change. All of the heating and cooling rates were 10 °C/min, and the sample weight was 30 mg. A Leitz optical polarized microscope Model BK-2 equipped with hot stage was used to observe the thermal transitions and to analyze the anisotropic textures.

The photolyses of the polymers were done in solutions as well as in films. For UV spectral studies, films were cast on the outer surface of a 1-cm quartz cuvette from chloroform solution. The film thickness was adjusted until an optical density (OD) between 1.0 and 1.5 was obtained. For studies on the FTIR spectrophotometer, a thin film of polymer was formed on one side of a KBr pellet of 10-mm diameter and 0.5-mm thickness. The film thickness was adjusted to obtain absorbance between 0.05 and 0.10. The photochemical studies were carried out in a discontinuous mode; i.e., the samples were exposed to UV radiation from a 125-W medium-pressure mercury lamp, kept at a distance of 10 cm from the sample for varying intervals of time. The irradiated films were subsequently subjected to spectral analysis.

Results and Discussion

Synthesis. The monomers, bis(4-hydroxybenzylidene)cycloalkanones, were prepared as described under Experimental Section by taking 2:1 molar ratio of p-hydroxybenzaldehyde and the corresponding cycloalkanone. Three different cycloalkanones, namely cyclopentanone, cyclohexanone, and cycloheptanone, were used. All three monomers are crystalline and melt to isotropic liquids. Tetragolic acid, a dicarboxylic acid, was prepared by the oxidation of tetraethylene glycol and converted to the corresponding diacid chloride using oxalyl chloride.

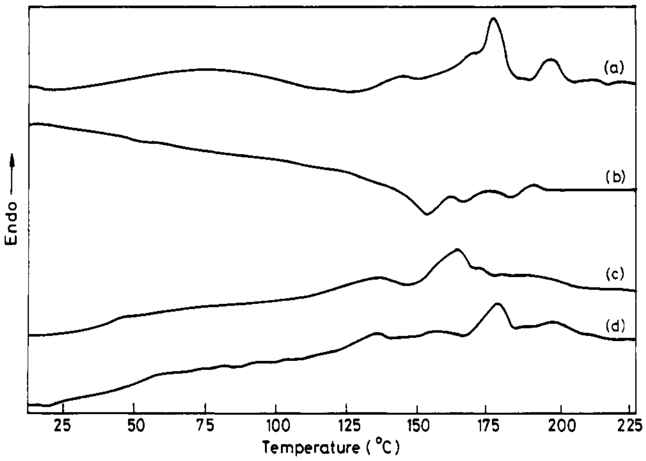

Figure 2. DSC thermograms of PMCLCP-02: (a) first heating cycle; (b) first cooling cycle; (c) second heating cycle; (d) heating cycle of the annealed sample (130 °C, 3 h).

Polymers with three different mesogenic structures (PMCLCP-02, PMCLCP-12, and PMCLCP-22) were synthesized by solution polycondensation, as shown in Scheme I. The yield, viscosity, and spectral data for these polymers are given in Tables I and II. A typical ^1H NMR spectra for PMCLCP-22 is shown in Figure 1. The bis(benzylidene)cycloalkanone chromophores, spaced periodically in the backbone, introduce photoreactivity, and the anisotropy of the shape imparts thermotropic behavior to the polymers. The ether linkages in the spacer units are expected to introduce greater flexibility to the polymer chains and consequently bring down the transition temperatures.

Liquid Crystalline Properties. The liquid crystalline properties of these polymers were studied by DSC and polarized optical microscopy (POM). The DSC thermograms are shown in Figures 2–4 and the results are summarized in Table III. The temperatures T_1, T_2, T_3, and T_i refer to the peak temperatures of the successive

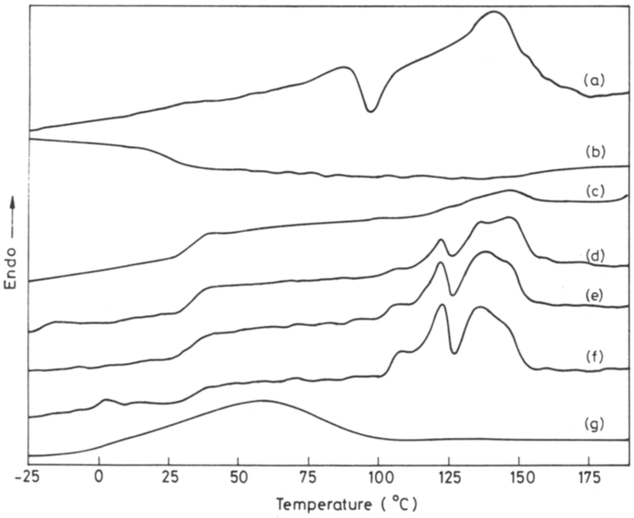

Figure 3. DSC thermograms of PMCLCP-12: (a) first heating cycle; (b) first cooling cycle; (c) second heating cycle; (d, e, f) heating cycles of the annealed sample at 90 °C for 15, 30, and 60 min, respectively; (g) heating scan after irradiation for 5 h.

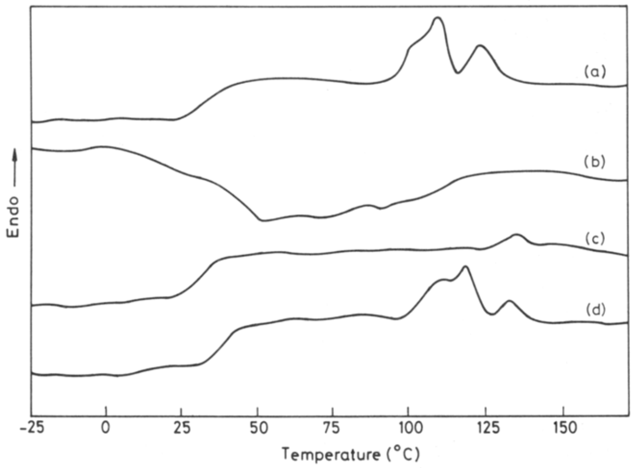

Figure 4. DSC thermograms of PMCLCP-22: (a) first heating cycle; (b) first cooling cycle; (c) second heating cycle; (d) heating cycle of the annealed sample (75 °C, 3 h).

Table III. Thermal Properties of the Polymers from DSC

polymer	transition temp, °C				
	T_g	T_1	T_2	T_3	T_i
PMCLCP-02		135	157	175	197
PMCLCP-12	36	106	123	137	148
PMCLCP-22	31		107	117	132

endotherms observed in the heating scan for the annealed samples. In general, for the highest transition temperature there is a single endotherm corresponding to the transition from the liquid crystalline to the isotropic state. The transition from crystal to liquid crystal gives rise to one or more endotherms;[40,41] the one occurring at the highest temperature is attributed to the crystal to mesophase transition. The POM studies show no evidence for fluidity below this temperature. The remaining lower temperature endotherms represent unidentified crystal to crystal transitions.

For PMCLCP-02 (Figure 2), the first heating scan (curve a) shows an endotherm at 172 °C for the melting to anisotropic liquid. This was preceded by two small endotherms as shoulders at 140 and 162 °C for the crystal to crystal transitions. The endotherm at 192 °C is for the isotropization. Examining the polymer in POM shows a fine schlieren texture, confirming the nematic mesophase in this polymer. In the first cooling cycle (curve b), there are three exotherms, at 173 °C for the isotropic to nematic transition and the remaining two at 155 and 143 °C for the crystallization. The second heating scan (curve c) also shows multiple endotherms for melting, as is seen in the first heating scan, but they have smaller enthalpies of transition. Curve d is for the heating cycle of the sample annealed at 150 °C for 3 h, after the second heating scan. It can be seen that annealing results in clear and well-separated transition peaks.

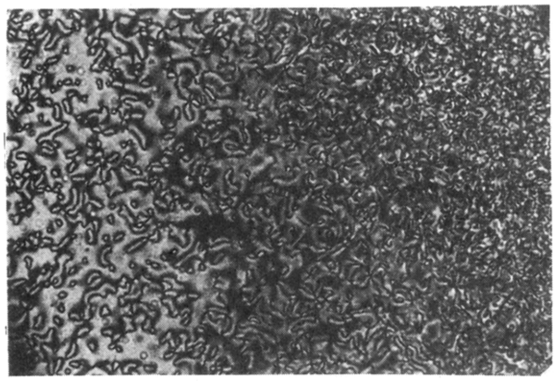

Figure 5. Optical polarization micrograph of PMCLCP-12 at 110 °C on cooling from isotropic phase.

For PMCLCP-12, the DSC thermograms are shown in Figure 3. In the first heating scan (curve a), there is a broad endotherm at 89 °C followed by an exotherm at 99 °C for the crystallization and another endotherm at 145 °C. POM study of this sample disclosed that the sample melts to anisotropic fluid at 120 °C and turns to complete isotropic liquid at 165 °C. In the first cooling scan (curve b), a small broad exotherm, centered at 135 °C, is observed for the transition from isotropic to anisotropic state. There is no exotherm for the crystallization. In fact, the POM studies confirm that the sample remains as anisotropic liquid down to T_g, below which it solidifies, retaining the LC texture, into the so-called LC glassy state. Figure 5 shows the microphotograph of PMCLCP-12 at 110 °C on cooling from the isotropic melt. The schlieren texture confirms the nematic mesomorphism in this polymer also. In the second heating scan (curve c), the polymer slowly transforms to nematic state above T_g and nematic to isotropic at 148 °C, represented by a small endotherm. No endotherm for melting was seen. However, annealing the sample at 95 °C induces the crystallization, and subsequent heating scans (curves d–f), at different annealing times, show endotherms at 107 °C for the crystal to crystal and at 124 °C for the crystal to nematic transitions. There are two overlapping endotherms at 137 and 149 °C. While the former is assigned to isotropization, the identification of the latter was rendered difficult since POM did not show any visible change at this temperature.

PMCLCP-22 also exhibits a nematic mesophase and shows a DSC behavior similar to that of PMCLCP-12 (Figure 4). It did not show a clear exotherm for crystallization on cooling (curve b) and corresponding endotherm for melting in the subsequent heating cycles (curve c) and requires annealing, below the melting temperature, to induce crystallization (curve d). The reason PMCLCP-12 and PMCLCP-22 fail to crystallize on cooling could be the change in the geometry of the bis(benzylidene)-cycloalkanone units of the polymer, which depends upon the size of the cycloalkanone ring. As the ring size increases, the mesogens slowly lose their linear rigid geometry and become semirigid rodlike, thus enhancing the flexibility of the polymer chains. In this situation not

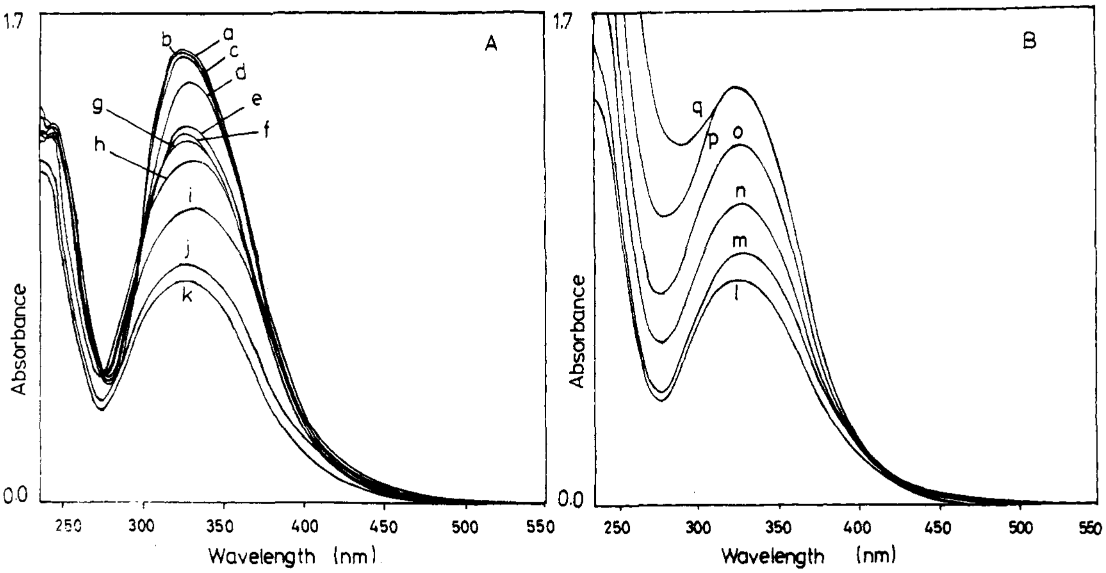

Figure 6. Thermal effect on UV absorption spectra of the PMCLCP-12 film: (A) (a) 20, (b) 30, (c) 40, (d) 50, (e) 60, (f) 70, (g) 90, (h) 100, (i) 110, (j) 120, and (k) 130 °C; (B) (l) 140, (m) 150, (n) 160, (o) 170, (p) 180, and (q) 200 °C.

only is the crystallization rendered difficult, eventually becoming kinetically controlled, but the transition temperatures also are lowered. The transition temperatures in these polymers are found to be drastically influenced by the thermal history of the sample. Hence, the transition temperatures from the heating cycle of the annealed samples are given in Table III.

Thermal Effect on the Polymer Film. The polymer film, formed by solvent casting, was heated, and the resultant thermal effect was monitored by analyzing the UV spectra as a function of temperature. Figure 6 shows the UV spectral pattern for PMCLCP-12 on heating from 20 to 200 °C at a rate of 5 °C/min. In the beginning, at 20 °C, the spectrum shows an absorption maxima at 322 nm for the $\pi \rightarrow \pi^*$ transition. On heating, no significant change in the spectrum is seen until the temperature reaches about 40 °C, above which the intensity of the 322-nm peak shows a rapid decrease up to 50 °C and thereafter it decreases gradually until 70 °C. Along with the decrease in the intensity, the peak is simultaneously broadened and shows a red shift. From 70 to 100 °C, the spectrum remains almost unchanged. On further heating, once again there was a decrease in intensity of the peak until the temperature reaches 120 °C. Between 120 and 140 °C, no appreciable change in the spectrum was seen, above which however, the intensity increases until 180 °C. Between 180 and 200 °C, the peak intensity again remains constant.

The temperatures associated with these intensity changes were correlated with the transition temperatures of the polymer. Figure 7 shows the plots of the variation of the intensity of the peak at 322 nm (curve a) and its first derivative (curve b) as a function of temperature on heating. The DSC heating thermogram (curve c) is also given for comparison. The derivative plot brings about the clear manifestation of the changes in the peak intensity for easy comparison with the transition temperatures observed in DSC. It can be seen that the first decrease in intensity (BD) occurs just after the glass transition of the polymer. The second stage of decrease (EF) starts at the crystal to crystal transition and continues until the polymer completely melts to the nematic phase. The increase in intensity (GH) is observed as the polymer changes to isotropic state. These changes in the UV spectra have been attributed to the varied arrangement of the chromophores[19] with heating of the polymer film between T_g and T_i.

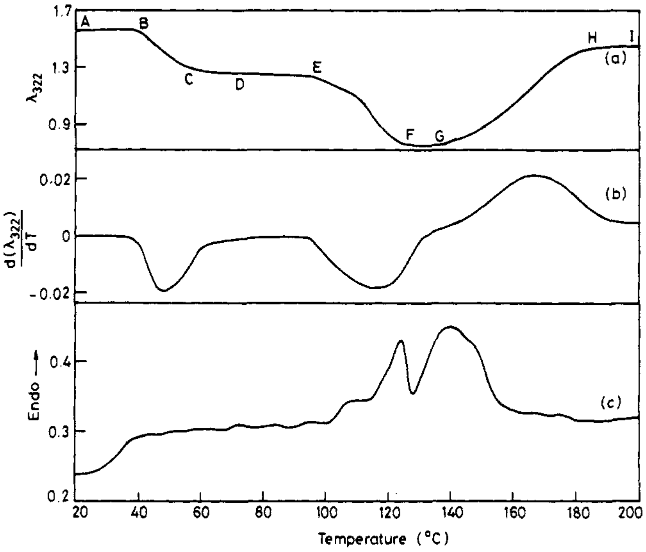

Figure 7. Thermal effect on UV absorption spectra for PMCLCP-12: (a) variation of intensity at 322-nm peak as a function of temperature; (b) differential plot of curve a; (c) DSC heating cycle of PMCLCP-12.

When the polymer film is cast from solution, the chromophores have mostly random orientation. The initial decrease in intensity when the film is heated above 40 °C is because of the parallel aggregation of the chromophores due to the inherent tendency of the mesogens to become ordered. This type of aggregation is facilitated above T_g because of the greater mobility of the polymer chains. The second decrease at 100 °C is for the further aggregation of the chromophores when the polymer changes from one crystalline form to another. This aggregation attains its optimum value as the polymer melts to the nematic phase. Obviously, this phenomenon of ordering on heating would be absent in an already ordered film. Indeed, the films annealed above T_g did not exhibit any such decrease in intensity on heating, as seen in Figure 8A.

The increase in intensity when the film is heated above the isotropic temperature is due to the change in the arrangements of the chromophores from ordered to random orientation. It may therefore be concluded that in this polymer the decrease in intensity reveals ordered aggregation, while an increase in intensity reflects the random orientation of the chromophores. When the

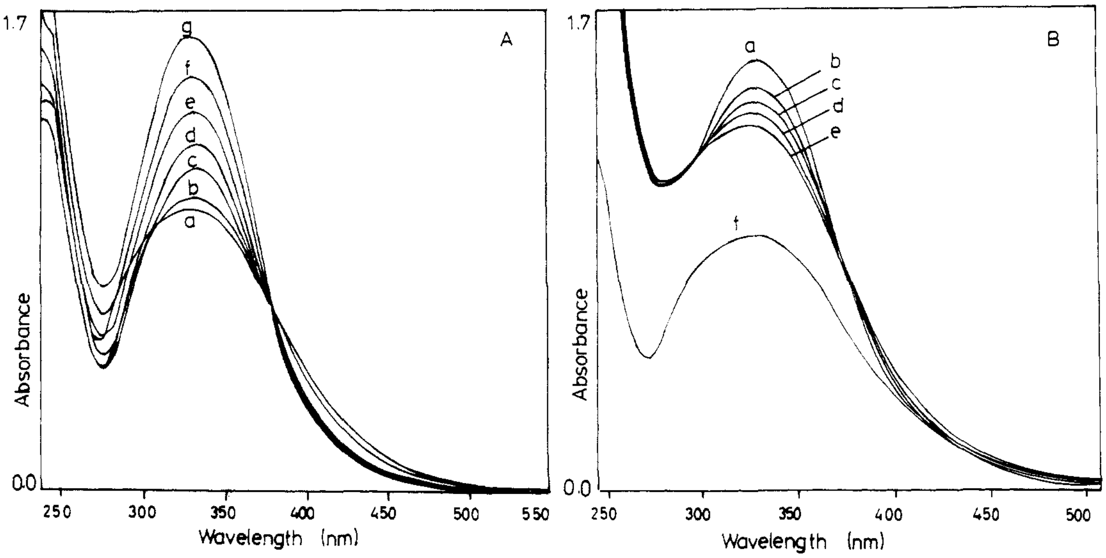

Figure 8. Thermal effect on UV absorption spectra of the PMCLCP-12 films: (A) annealed at 90 °C for 3 h, (a) 20, (b) 60, (c) 100, (d) 120, (e) 130, (f) 140, and (g) 150 °C; (B) on cooling from the isotropic phase, (a) 180, (b) 130, (c) 110, (d) 60, (e) 20, and (f) 20 °C, after annealing at 90 °C for 3 h.

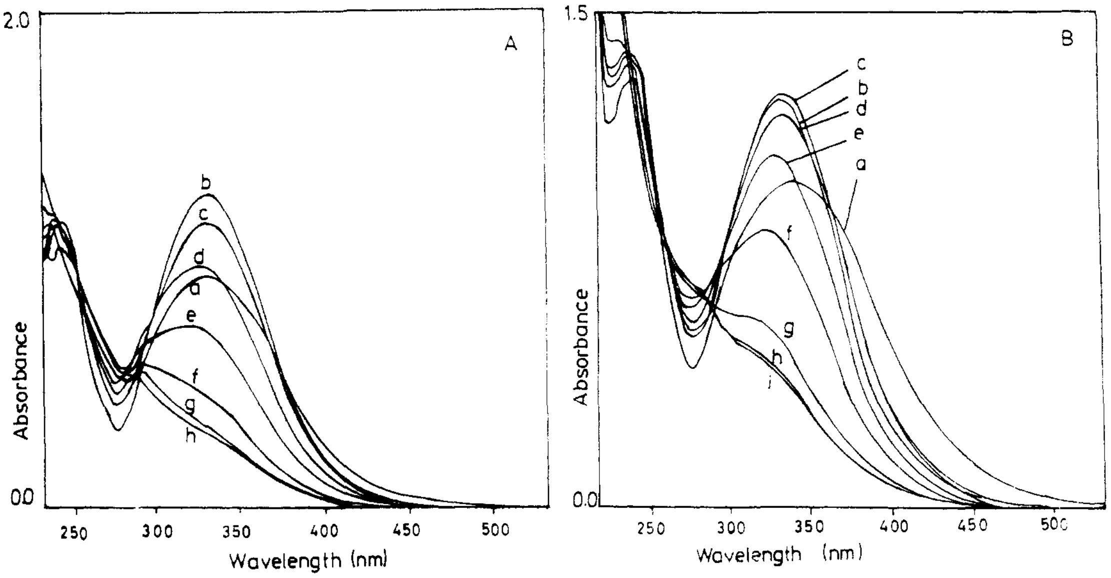

Figure 9. Change in UV spectral characteristics during the photolysis of PMCLCP-12 films for different time intervals: (A) at 130 °C, (a) 0, (b) 0.5, (c) 1, (d) 2, (e) 4, (f) 8, (g) 15, and (h) 15 min, after the irradiated film was washed with chloroform; (B) at 75 °C, (a) 0, (b) 0.5, (c) 1, (d) 3, (e) 6, (f) 15, (g) 30, (h) 80, and (i) 80 min, after the irradiated film was washed with chloroform.

polymer is cooled from the isotropic state, one would expect a decrease in UV intensity as the polymer enters into the nematic phase. In fact, a decrease in intensity, but of smaller magnitude, was observed (Figure 8B). This may be due to the incomplete aggregation of the chromophores on cooling. This is corroborated by the observation of a very weak and broad exotherm for the isotropic to nematic transition and complete absence of the crystallization exotherm in the DSC cooling scan (Figure 3, curve b). Annealing this film at 90 °C for 3 h restores the full aggregation of the chromophores, which is reflected in the similarity of the UV spectra (Figure 8B, curve f) with that of the aggregated one (Figure 8A, curve a).

Photolysis of the Polymers. The polymer films were subjected to photolysis and the structural changes were followed by UV and IR spectra. Figure 9A shows a series of UV spectra for PMCLCP-12 film for different time intervals of irradiation at 130 °C, in the nematic phase. There is an increase in the intensity as well as a small blue shift for the 322-nm peak, at the first 0.5 min of irradiation (curve b). This increase in intensity reverses on further irradiation and decreases regularly thereafter. After 15 min of irradiation, the peak at 322 nm completely disappears and a new peak emerges at 287 nm (curve g). The insolubility of the film at this stage of photolysis and the similarity of the UV spectra before and after washing with chloroform (curve h) indicate that the polymer has undergone cross-linking by irradiation.

The increase in the intensity of the 322-nm peak at the initial stages of irradiation was also observed when the photolysis was done at 75 °C, as shown in Figure 9B. The explanation for this increase in the intensity can be derived from the results obtained on the thermal treatment of the polymer film, discussed earlier. There, the increase in intensity has been assigned to the disorganization caused by the randomly oriented bis(benzylidene)cycloalkanone chromophores as the polymer changes to the isotropic state. Such a disordered structure could also be introduced by the trans to cis photoisomerization of the bis(benzylidene)cyclohexanone chromophores on irradiation. This kind of isomerization, well-known in similar low molecular weight compounds,[42-44] can disrupt the parallel stacking of the chromophores in the aggregate because of the nonlinear conformation of the cis isomer. Interestingly,

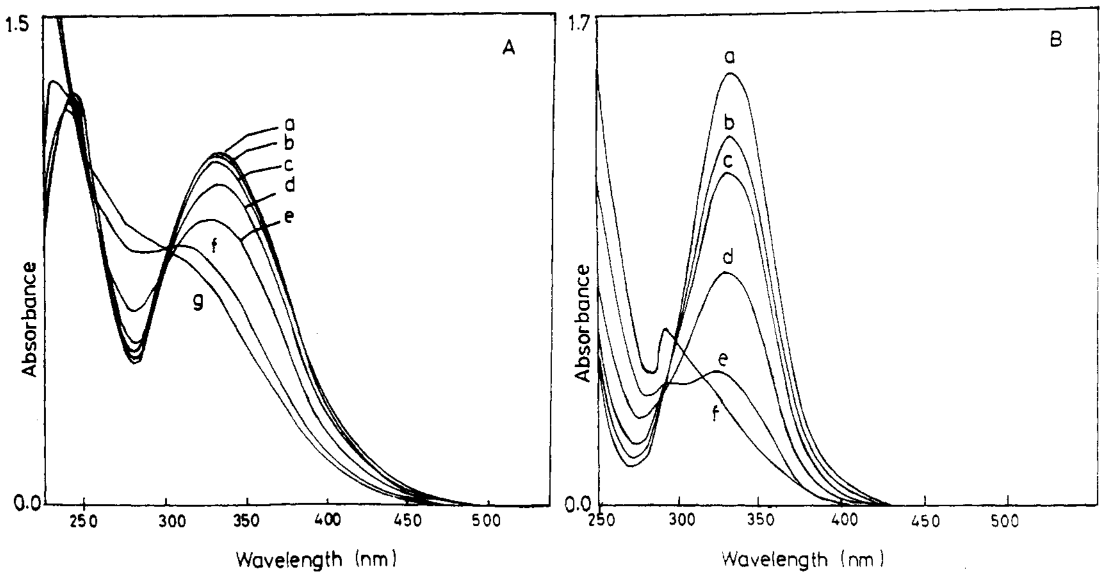

Figure 10. Change in UV spectral characteristics during photolysis of PMCLCP-12 film at 25 °C for different time intervals: (A) in film, (a) 0, (b) 0.5, (c) 1, (d) 10, (e) 40, and (f) 160 min; (B) in chloroform solution, (a) 0, (b) 0.5, (c) 1, (d) 3, (e) 5, and (f) 9 min.

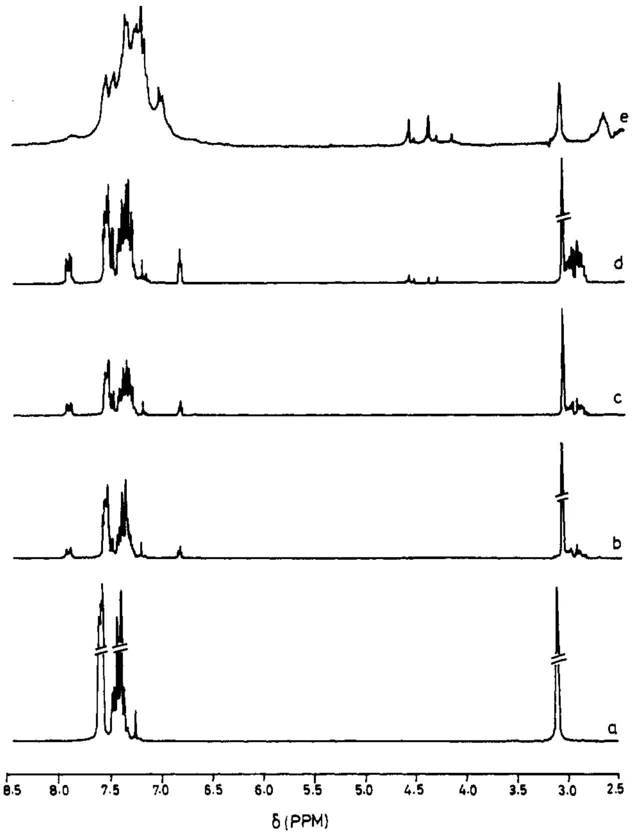

Figure 11. ^{1}H NMR spectra of bis(benzylidene)cyclopentanone in $CDCl_3$ during photolysis: (a) 0, (b) 5, (c) 15, and (d) 30 min, all in chloroform solution; (e) 5 h in solid state.

Scheme II. Photochemical Reactions of Bis(benzylidene)cyclopentanone

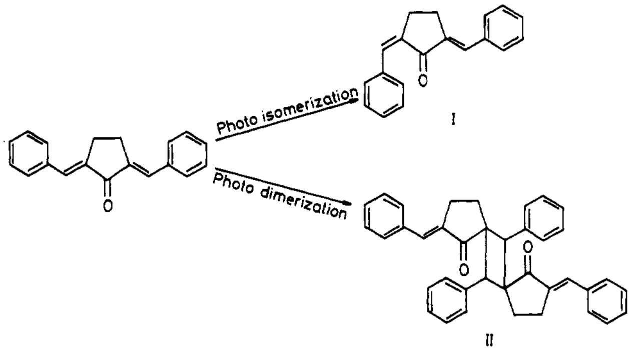

there was no increase in the intensity at the initial stages of photolysis for the polymer film, below T_g, as well as for the polymer in solution; instead, a regular decrease with the irradiation time was observed (Figure 10). This is understandable because the photoisomerization is less likely to occur below T_g, in a rigid glassy state, due to the restricted motion of the chains in the polymer film. In the case of polymer in solution, although the photoisomerization cannot be ruled out, the question of disruption of chromophore aggregate does not arise since there is no ordered arrangement of the chromophores in solution.

The decrease in the intensity of the 322-nm peak and the appearance of a new peak at 287 nm at the later stages of photolysis (Figure 9A) have been attributed to the cross-linking reactions involving bis(benzylidene)cycloalkanone chromophores. Further support for the occurrence of cross-linking was obtained from DSC measurements of the irradiated polymer. In Figure 3, curve g shows the DSC heating thermogram of the PMCLCP-12 film irradiated for 5 h. Only one broad endothermic process corresponding to the glass transition was seen. It is clear that the T_g of the polymer is shifted to a higher temperature, indicative of cross-linking, and the melting and nematic to isotropic transitions disappeared. The simultaneous irradiation and examination of PMCLCP-12 in POM reveals that in the mesophase, in addition to the increase in viscosity due to the cross-linking, a partial loss of birefringence also occurs. In the glassy state, although the polymer undergoes cross-linking, the nematic texture remains undisturbed.

To gain further insight into the mechanism of the photoreactions, a study on the model compound, bis(benzylidene)cyclopentanone, has been carried out. Under the influence of light, this compound undergoes two kinds of reactions, namely the trans–cis isomerization[42] and $2\pi + 2\pi$ cycloaddition leading to the dimer formation[45–48] (Scheme II). Figure 11 shows the ^{1}H NMR spectra of this model compound for the photolysis in solution as well as in the solid state. For the sample irradiated in solution, a peak corresponding to the *exo*-olefinic protons of cis isomer is observed at 6.89 ppm and will grow in intensity with time, for the first 15 min. Upon further irradiation, new peaks appear near 4.5 ppm for the cyclobutane protons of the dimer. When the irradiation was done in the solid

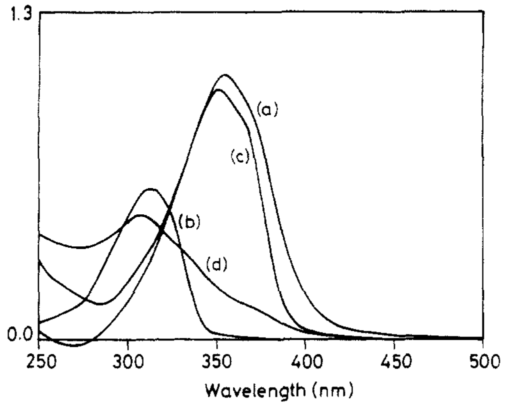

Figure 12. UV absorption spectra in chloroform: (a) PMCLCP-02, before cross-linking; (b) PMCLCP-02, after cross-linking; (c) bis(benzylidene)cyclopentanone; (d) photodimer bis(benzylidene)cyclopentanone.

state, the peaks were seen only for the dimer and not for the cis isomer. Since the polymer chains are mobile only above T_g, the photoisomerization and photo-cross-linking in the polymers can be compared with the photoisomerization and photodimerization, respectively, observed for the model compound in the solution. In the model compound, the photoisomerization, being faster, supersedes the photodimerization, which occurs only at the later stages of the irradiation. The disruption of the parallel stacking of the mesogens as a result of trans–cis photoisomerization and fading of the birefringence with irradiation leads us to propose that there is some degree of radiation-induced transition to the isotropic state when photolysis is done in the nematic phase.

The photodimer II has been isolated and compared with the cross-linked polymer. Figure 12 shows the UV spectra for PMCLCP-02 before and after the irradiation and also the spectra of the bis(benzylidene)cyclopentanone and its dimer. The close similarity between the spectra of the unirradiated polymer and the model compound, on the one hand, and the irradiated polymer and the photodimer of the model compound, on the other, proves that the $2\pi + 2\pi$ cycloaddition of the bis(benzylidene)cyclopentanone units present in the polymer backbone leads to the cross-linking. Further supporting evidence for these photo-cross-linking reactions was obtained from FTIR studies on this polymer.

Figure 13 shows the changes in the IR absorption bands on irradiation of the PMCLCP-02. A decrease in absorbance is observed for the $\nu_{C=C}$ band at 1602 cm^{-1}. The decrease is maximum for the first 0.5 min of irradiation. Simultaneously, there is a shift toward higher wavenumber for the $\nu_{C=O}$ band at 1700 cm^{-1} due to the breaking of conjugation in the bis(benzylidene)cyclopentanone units during the cross-linking.

It is of interest to compare the rate of cross-linking among the polymers of different mesogenic structures. This is done by monitering the $2\pi + 2\pi$ cycloaddition reactions through the decrease in the intensity of the $\nu_{C=C}$ band during photolysis. The intensity of this band was normalized with respect to that of the ν_{C-H} asymmetric stretching band at 1295 cm^{-1}. In Figure 14, the relative photochemical reactivity, $(A_0 - A_t)/A_0$, is plotted against time of irradiation for the three polymers, where A_t is the absorbance of the $\nu_{C=C}$ band after irradiation for time t and $A_0 = A_t$ when $t = 0$. PMCLCP-02 is found to be the most reactive and PMCLCP-22 the least, while PMCLCP-12 shows intermediate reactivity. In PMCLCP-02, about 80% of the conversion takes place in the first minute of irradiation. This trend in the photoreactivity may be attributed to the unfavorable geometry of the bis(benzylidene)cycloalkanone for the $2\pi + 2\pi$ cycloaddition, which is rendered difficult with the increase in cycloalkanone ring size.

Figure 15 shows the plot of photochemical reactivity as a function of temperature for PMCLCP-12, for a fixed 0.5 min of irradiation. The photoreactivity is low below 40 °C; above this temperature there is an increase until 80 °C, and then it remains constant up to around 130 °C. At 140 °C and above there is a sudden decrease in the rate of cross-linking. The increase of cross-linking rate above 40 °C is due to the aggregation of the chromophores, as discussed in the thermal treatment of the film. This aggregation facilitates the cycloaddition reactions. The drastic decrease of cross-linking rate above 140 °C is explained by the fact that the polymer changes from nematic to isotropic phase near this temperature where

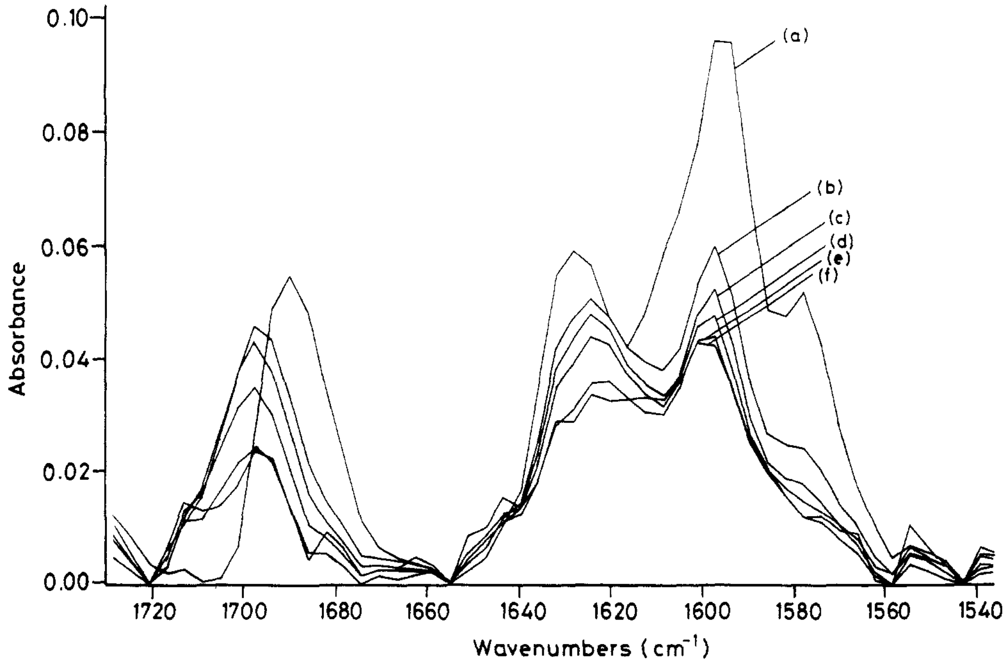

Figure 13. Change in IR spectral characteristics of PMCLCP-02 film on irradiation: (a) 0, (b) 0.5, (c) 1, (d) 3, (e) 10, and (f) 20 min.

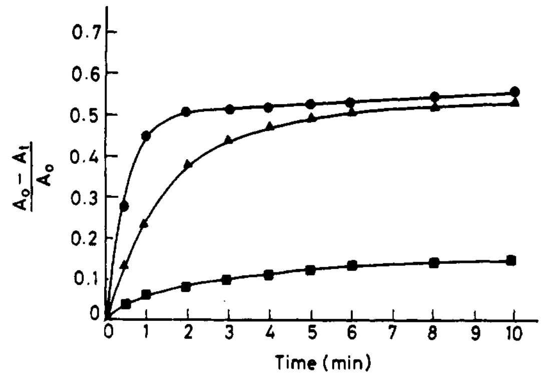

Figure 14. Dependence of photo-cross-linking rate on irradiation time: (●) PMCLCP-02; (▲) PMCLCP-12; (■) PMCLCP-22.

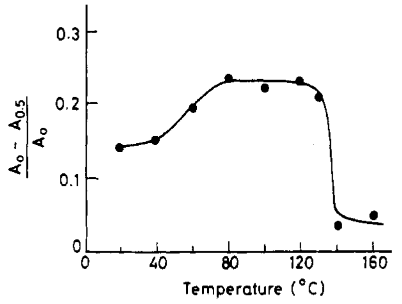

Figure 15. Temperature dependence of photochemical reactivity in PMCLCP-12.

random orientation of the chromophores does not favor the cycloaddition reaction.

Conclusions

The present study has brought into focus a new class of photo-cross-linkable LCPs derived from bis(4-hydroxybenzylidene)cycloalkanones and tetragolic acid. Here, the photoreactivity can be suitably controlled by modifying the structure by the proper selection of cycloalkanone. These polymer systems do not show any side reactions, unlike the photo-cross-linkable LCPs based on the cinnamate esters, where photo-Fries rearrangement gives undesirable byproducts. These polymers may be potentially useful in the poling of nonlinear optical materials (NLOs). The mesophase-mediated poling promotes the easy orientation of NLOs in the magnetic field,[30] and the ability of the polymers to undergo cross-linking can be utilized to permanently freeze-in the oriented NLOs after the poling.[49] The inherent 'polymeric' nature can be conveniently used for making films, coatings, etc. The trans to cis photoisomerization of the chromophores disrupts the ordered aggregates of the mesogen and results in the optical contrast between irradiated and unirradiated portions.[28,29] This phenomenon can be suitably exploited for developing information storage devices. Another attractive feature of this study is the illustration as to how the phenomenon of organization of chromophores affects the photochemical behavior of polymers.

Acknowledgment. We are thankful to Prof. N. V. Madhusudhana, Raman Research Institute, Bangalore, for providing the POM facility and the Department of Science and Technology, New Delhi, for financial support.

References and Notes

(1) Roviello, A.; Siragu, A. *J. Polym. Sci., Polym. Lett. Ed.* **1975**, *13*, 455.
(2) *Recent Advances in Liquid Crystalline Polymers*; Chapoy, L. L., Ed.; Elsevier Applied Science: London, 1985.
(3) *Side chain liquid crystalline polymers*; McArdle, C. B., Ed.; Chapman and Hall: New York, 1989.
(4) Hani, R.; Lenz, R. W. *Silicon based polymer science, A Comprehensive Resource*; Advances in Chemistry Series 224; American Chemical Society: Washington DC, 1990; p 741.
(5) Hikmet, R. A. M.; Lub, J.; Broer, D. J. *Adv. Mater.* **1991**, *3*, 392.
(6) Barclay, G. G.; McNamec, S. G.; Ober, C. K.; Parathomas, K. I.; Wang, D. W. *J. Polym. Sci., Polym. Chem. Ed.* **1992**, *30*, 1845.
(7) Finkelman, H. *Angew. Chem.* **1988**, *100*, 1019.
(8) Schatzle, J.; Kaufhold, W.; Finkelman, H. *Makromol. Chem.* **1989**, *190*, 3269.
(9) Zentel, R. *Liq. Cryst.* **1986**, *1*, 589.
(10) Barnes, N. R.; David, S. J.; Mitchell, G. R. *Mol. Cryst. Liq. Cryst.* **1989**, *168*, 13.
(11) Davis, F. J.; Mitchell, G. R. *Polym. Commun.* **1987**, *28*, 8.
(12) Mitchell, G. R.; Davis, F. J.; Ashman, A. S. *Polymer* **1987**, *28*, 639.
(13) Kock, H. J.; Finkelman, H.; Gleem, W.; Rehage, G. In *Polymer Science and Technology*; Blumstein, A., Ed.; Plenum: New York, 1983; Vol. 28.
(14) Heynderickx, I.; Broer, D. J. *Mol. Cryst. Liq. Cryst.* **1991**, *203*, 113.
(15) Davis, F. J.; Gilbert, A.; Mann, J.; Mitchell, G. R. *J. Chem. Soc., Chem. Commun.* **1986**, 1333.
(16) Broer, D. J.; Finkelman, H.; Kondo, K. *Makromol. Chem.* **1985**, *189*, 185.
(17) Broer, D. J.; Mol, G. N. *Makromol. Chem.* **1989**, *190*, 19.
(18) Broer, D. J.; Heynderickx, I. *Macromolecules* **1990**, *23*, 2474.
(19) Greed, D.; Griffin, A. C.; Gross, J. R. D.; Hoyle, G. E.; Venketaraman, K. *Mol. Cryst. Liq. Cryst.* **1988**, *155*, 57.
(20) Keller, P. *Chem. Mater.* **1990**, *2*, 3.
(21) Whitcombe, M. J.; Gilbert, A.; Hirai, A.; Mitchell, G. R. *J. Polym. Sci., Polym. Chem. Ed.* **1991**, *29*, 251.
(22) Whitcombe, M. J.; Gilbert, A.; Mitchell, G. R. *Br. Polym. J.* **1990**, *23*, 77.
(23) Zentel, R.; Benalia, M. *Makromol. Chem.* **1987**, *188*, 665.
(24) Finkelman, H.; Kock, H.; Rehage, G. *Makromol. Chem., Rapid Commun.* **1981**, *2*, 317.
(25) Finkelman, H.; Kock, H.; Gleem, W.; Rehage, G. *Makromol. Chem., Rapid Commun.* **1984**, *5*, 287.
(26) Hitmet, R. A. M.; Broer, D. J. *Integration of Fundamental Polymer Science and Technology*; Kleinties, L. A., Lemstra, P., Eds.; Elsevier Applied Science: London, 1989.
(27) Broer, D. J.; Boven, J.; Mol, G. N.; Challa, G. *Makromol. Chem.* **1989**, *190*, 2255.
(28) Griffin, A. C.; Hoyle, C. E.; Gross, J. R. D.; Venkataram, K.; Creed, D.; McArdly, C. B. *Makromol. Chem.* **1988**, *9*, 463.
(29) Legge, C. H.; Whitcombe, M. J.; Gilbert, A.; Mitchell, G. R. *J. Mater. Chem.* **1991**, *1*, 303.
(30) Ulrich, D. R. *Mol. Cryst. Liq. Cryst.* **1990**, *189*, 3.
(31) Creed, D.; Griffin, A. C.; Hoyle, C. H.; Venkatram, K. *J. Am. Chem. Soc.* **1990**, *112*, 4049.
(32) Nonan, J. M.; Caccamo, A. F. *Polym. Prepr. (Am. Chem. Soc., Div. Polym. Chem.)* **1984**, *30*, 501.
(33) Koch, T.; Ritter, H.; Buchholz, N. *Makromol. Chem.* **1989**, *190*, 1369.
(34) Loth, H.; Euschem, A. *Makromol. Chem., Rapid. Commun.* **1988**, *9*, 35.
(35) Krigbaum, W. R.; Ishikawa, T.; Watanabe, J.; Torium, H.; Kubota, K. *J. Polym. Sci., Polym. Chem. Ed.* **1983**, *21*, 1851.
(36) Peter, K.; Ratzsch, M. *Makromol. Chem.* **1990**, *191*, 1021.
(37) Whitcombe, M. J.; Gilbert, A.; Mitchell, G. R. *J. Polym. Sci., Polym. Chem. Ed.* **1992**, *30*, 1681.
(38) Iketa, T.; Itakura, H.; Lee, C.; Winnik, F. M.; Tazuke, S. *Macromolecules* **1988**, *21*, 3537.
(39) Adams, R.; Noller, C. R. *Organic Syntheses*; Wiley: New York, 1941; Collect. Vol. I, p 192.
(40) Cheng, S. Z. D. *Macromolecules* **1988**, *21*, 2475.
(41) Cheng, S. Z. D.; Zhang, A.; Johnson, R. L.; Zhou, Z. *Macromolecules* **1989**, *22*, 4292.
(42) George, H.; Roth, H. T. *Tetrahedron Lett.* **1971**, *43*, 4057.
(43) Aizeshtat, Z.; Hausmann, M.; Pickholtz, Y.; Tal, D.; Blum, J. *J. Org. Chem.* **1977**, *42*, 2386.
(44) Wargnier, F. B.; Feigenbaum, A.; Mutzart, J. *J. Chem. Educ.* **1978**, *55*, 339.
(45) Forward, G. C.; Whiting, A. G. *J. Chem. Soc. C* **1969**, 1868.
(46) Frey, H.; Behman, G.; Kaupp, G. *Chem. Ber.* **1987**, *120*, 387.
(47) Zimmermann, I.; Kaupp, G. *Angew. Chem., Int. Ed. Engl.* **1981**, *20*, 1018.
(48) Theocharis, C. R.; Jones, W.; Thomas, M. J.; Molevalli, M.; Hursthouse, B. M. *J. Chem. Soc., Perkin Trans. 2* **1984**, 71.
(49) Chen, M.; Yu, L.; Dalton, L. R. *Macromolecules* **1991**, *24*, 5421.